Interaction of the N-Terminal Domain of Apolipoprotein E4 with Heparin†

Jun Dong,‡ Clare A. Peters-Libeu,‡,§ Karl H. Weisgraber,‡,§,|| Brent W. Segelke,⊥ Bernhard Rupp,⊥ Ishan Capila,@ Maria J. Hernáiz,@ Laurie A. LeBrun,@ and Robert J. Linhardt*,@

Gladstone Institute of Cardiovascular Disease, Cardiovascular Research Institute, and Department of Pathology, University of California, San Francisco, California 94941-9100, Lawrence Livermore National Laboratory, Biology and Biotechnology Research Program, L-452, University of California, Livermore, California 94550, and Departments of Chemistry, Medicinal and Natural Products Chemistry, and Chemical and Biochemical Engineering, University of Iowa, Iowa City, Iowa 52242

Received October 17, 2000; Revised Manuscript Received December 15, 2000

ABSTRACT: Apolipoprotein E (apoE) is an important lipid-transport protein in human plasma and brain. It has three common isoforms (apoE2, apoE3, and apoE4). ApoE is a major genetic risk factor in heart disease and in neurodegenerative disease, including Alzheimer's disease. The interaction of apoE with heparan sulfate proteoglycans plays an important role in lipoprotein remnant uptake and likely in atherogenesis and Alzheimer's disease. Here we report our studies of the interaction of the N-terminal domain of apoE4 (residues 1−191), which contains the major heparin-binding site, with an enzymatically prepared heparin oligosaccharide. Identified by its high affinity for the N-terminal domain of apoE4, this oligosaccharide was determined to be an octasaccharide of the structure ΔUAp2S(1→[4)-α-D-GlcNpS6S-(1→4)-α-L-IdoAp2S(1→]$_3$4)-α-D-GlcNpS6S by nuclear magnetic resonance spectroscopy, capillary electrophoresis, and polyacrylamide gel electrophoresis. Kinetic analysis of the interaction between the N-terminal apoE4 fragment and immobilized heparin by surface plasmon resonance yielded a K_d of 150 nM. A similar binding constant (K_d = 140 nM) was observed for the interaction between immobilized N-terminal apoE4 and the octasaccharide. Isothermal titration calorimetry revealed a K_d of 75 nM for the interaction of the N-terminal apoE fragment and the octasaccharide with a binding stoichiometry of approximately 1:1. Using previous studies and molecular modeling, we propose a binding site for this octasaccharide in a basic residue-rich region of helix 4 of the N-terminal fragment. From the X-ray crystal structure of the N-terminal apoE4, we predicted that binding of the octasaccharide at this site would result in a change in intrinsic fluorescence. This prediction was confirmed experimentally by an observed increase in fluorescence intensity with octasaccharide binding corresponding to a K_d of ∼1 μM.

Apolipoprotein E (apoE)[1] is an important lipid-transport protein in human plasma and brain. In recent years, biochemical, cell biological, and epidemiological studies have suggested that apoE is a major genetic risk factor in a number of diseases (*1*). The human *APOE* gene has three common alleles (ε2, ε3, and ε4). The three isoforms differ at amino acids 112 and 158 and vary in their metabolic properties and association with disease (*1*). ApoE3 (Cys-112 and Arg-158), the most common isoform, binds normally to LDL receptors and is associated with normal lipid metabolism, whereas apoE2 (Cys-112 and Cys-158) binds defectively and is associated with type III hyperlipoproteinemia (*2*). ApoE4 (Arg-112 and Arg-158) is associated with a higher risk of heart disease (*3*, *4*) and is a major genetic risk factor for Alzheimer's disease (*5*−*7*).

ApoE, a 299-residue, single-chain protein, contains two structural domains: an N-terminal domain and a C-terminal domain (*8*, *9*). As shown by X-ray crystallography, the N-terminal domain (residues 1−191) is composed of four amphipathic α-helices arranged in antiparallel fashion and connected by loop regions (*10*). The N-terminal domain contains the low-density lipoprotein (LDL) receptor-binding region (residues 136−150 of helix 4) (*11*). This region is characterized by a high concentration of basic amino acids and contains no acidic residues. The interaction with the LDL receptor is thought to be a complementary charge interaction between the basic residues in the receptor-binding region of apoE and the clusters of acidic residues in the seven cysteine-rich repeating units that constitute the ligand-binding domain

† The study was funded, in part, by grants from the National Institutes of Health (GM 38060 and HL 52622 to R.J.L. and HL 41633 and NS 35939 to K.H.W.). Lawrence Livermore National Laboratory is operated by the University of California for the U.S. Department of Energy under Contract W-7405-ENG-48.

* To whom correspondence should be addressed: Departments of Chemistry, Medicinal and Natural Products Chemistry, and Chemical and Biochemical Engineering, University of Iowa, Iowa City, IA 52242.

‡ Gladstone Institute of Cardiovascular Disease, University of California.

§ Cardiovascular Research Institute, University of California.

|| Department of Pathology, University of California.

⊥ Lawrence Livermore National Laboratory, Biology and Biotechnology Research Program, University of California.

@ University of Iowa.

[1] Abbreviations: apoE, apolipoprotein; SPR, surface plasmon resonance; ITC, isothermal titration calorimetry; CE, capillary electrophoresis; K_d, dissociation constant; ΔUAp, 4-deoxy-α-L-*threo*-hex-4-enopyranosyluronic acid; IdoAp, idopyranosyluronic acid; GlcAp, glucopyranosyluronic acid; GlcN, 2-aminoglucopyranose; S, sulfate; HSPG, heparan sulfate proteoglycan; LDL, low-density lipoprotein; MWCO, molecular weight cutoff; dp, degree of polarization; SAX-HPLC, strong anion exchange high-performance liquid chromatography.

10.1021/bi002417n CCC: $20.00
Published on Web 02/01/2001

of the LDL receptor (*12*). The structure of the C-terminal domain (residues 216−299) is not known, but has been predicted to be α-helical (*13*). The C-terminal domain contains the major lipid-binding elements and is responsible for the self-association of apoE in the absence of lipid (*11*, *14*).

Both the N- and C-terminal domains contain a heparin-binding site (*15*, *16*). The N-terminal domain contains a high-affinity heparin-binding site (residues 142−147) overlapping with the receptor-binding region (*16*). The C-terminal domain contains a heparin-binding site that is only available for interaction in the lipid-free state (*16*). A third heparin-binding site (residues 211−218) has been proposed for the segment of protein that connects the N-terminal and C-terminal domains (*15*).

Binding between glycosaminoglycans and other macromolecules has been hypothesized to have highly diverse functional roles, such as the structural organization of the extracellular matrix in connective tissue, the control of homeostasis, the specific binding of plasma proteins to the blood vessel wall, complement activation, and the regulation of cell behavior and metabolism (*17*, *18*). ApoE binds LDL receptors and plays a central role in plasma lipoprotein metabolism and cholesterol transport (*12*). In the liver, apoE mediates lipoprotein remnant binding to the heparan sulfate proteoglycan (HSPG)−LDL receptor-related protein pathway, facilitating lipoprotein uptake (*19*).

Most recently, the role of apoE and HSPG in the brain has come under increased scrutiny (*1*). Studies of cultured neurons suggest that the effects of Alzheimer's disease are mediated by the interaction of apoE with the HSPG−LDL receptor-related protein pathway (*19*). Neuro-2a cells treated with heparinase, which removes heparan sulfate chains from HSPG or chlorate, which blocks HSPG sulfation, do not show apoE3-induced neurite extension and apoE4-induced inhibition of neurite extension. Thus, the HSPG−LDL receptor-related protein pathway is essential for the observed apoE isoform-specific effects on neurite extension. According to this model, apoE interacts with the HSPG on the cell surface initially and is then transferred to the LDL receptor-related protein receptor for internalization. Thus, the interaction with glycosaminoglycans represents the initial recognition step that localizes the apoE to the cell surface.

Here we report our studies on the interaction between a heparin-derived oligosaccharide and the N-terminal domain of apoE4.

EXPERIMENTAL PROCEDURES

Preparation of the Heparin-Derived Octasaccharide. The heparin-derived octasaccharide was prepared from porcine intestinal mucosal heparin (145 IU/mg, Hepar Industries) by controlled enzymatic depolymerization with heparin lyase I (EC 4.2.2.7, Sigma Chemical Co.) as previously described (*20*). Briefly, 25 g of heparin was prepared in 400 mL of 50 mM sodium phosphate buffer (pH 7.0) containing 2 mg/mL bovine serum albumin (Sigma Chemical Co.) and sterilized with a filter (0.22 μm). To this solution was added 2.5 IU of heparin lyase I at time 0 and again at 24 h, and the mixture was incubated at 30 °C until the digestion was 50% complete. The mixture was adjusted to pH 3 with concentrated hydrochloric acid. The precipitated protein was removed by centrifugation, and the solution was passed through a sulfopropyl−Sephadex column to remove the remaining protein. The oligosaccharide mixture was adjusted to pH 7.0, freeze-dried, redissolved in water, and separated by pressure filtration with a 5000 molecular weight cutoff (MWCO) membrane (Millipore) into low-molecular weight (M_r < 5000) and high-molecular weight (M_r > 5000) oligosaccharides. The resulting low-molecular weight oligosaccharide mixture in 1 g/50 mL portions was fractionated on a 4.8 cm × 100 cm column packed with Sephadex G-50 (superfine, Pharmacia) and eluted with 50 mM sodium phosphate buffer (pH 7) containing 200 mM NaCl. The resulting oligosaccharide fractions, corresponding to mixtures of tetrasaccharides, hexasaccharides, and octasaccharides, were dialyzed (500 MWCO for tetra- and hexasaccharides and 1000 MWCO for octasaccharides) exhaustively against water and freeze-dried.

The apoE 22 kDa fragment (20 mg) was immobilized on 1.5 g of cyanogen bromide-activated Sepharose 4B (Pharmacia) according to the manufacturer's instructions. After this matrix was thoroughly washed, a 1 cm × 5 cm column was packed and equilibrated with 25 mM Gly-Gly buffer (pH 7.5). Tetrasaccharide-, hexasaccharide-, and octasaccharide-sized mixtures were individually loaded onto this affinity column washed with 10−20 column volumes of Gly-Gly buffer, and eluted by washing with a gradient from 75 mM to 1 M NaCl in the same buffer. High-affinity fractions (>150 mM NaCl eluent), prepared from each mixture, were desalted by dialysis as described above.

Oligosaccharide mixtures and high-affinity fractions prepared from the same mixtures were analyzed by strong anion exchange high-performance liquid chromatography (SAX-HPLC) at a flow rate of 4 mL/min on a 4.6 mm × 100 mm HQ/H SAX column (BioCAD) eluted with a 0 to 3 M linear NaCl gradient over the course of 22 min. The hexasaccharide-sized fraction eluted as two peaks, which were identified by coelution from a SAX-HPLC column with standards previously prepared in our laboratory (*20*). The octasaccharide-sized fraction with a high affinity for apoE eluted as a single peak, which was co-injected with the octasaccharide-sized mixture to identify the high-affinity component in this mixture. Repetitive fractionation with the same SAX column yielded the high-apoE affinity octasaccharide in the multi-milligram amounts required for structural characterization and interaction studies.

Electrophoresis Analysis of the Heparin Octasaccharide. The heparin octasaccharide was analyzed by polyacrylamide gel electrophoresis on a 22% polyacrylamide gel and visualized with alcian blue staining (*20*). Capillary electrophoresis (CE) analysis was performed on an ISCO CE system equipped with an ultraviolet detector set at 232 nm. The sample was applied at the cathode and subjected to reverse polarity with 20 mM phosphoric acid, adjusted to pH 3.5 with saturated dibasic sodium phosphate (*21*). Separation and analysis were carried out in a fused silica (externally coated except where the tube passed through the detector) capillary tube (50 μm inner diameter, 360 μm outer diameter, 62 cm long, and 42 cm effective length). The tube was washed extensively with 0.5 M sodium hydroxide, deionized distilled water, and running buffer. Samples were injected by vacuum injection (vacuum level 2, 12.79 kPa). Each experiment was performed at a constant voltage of 20 kV.

Characterization of the Heparin Octasaccharide. The octasaccharide sample (1 mg) was dissolved in D_2O (99%) and freeze-dried to remove exchangeable protons. After the sample was exchanged three times, it was dissolved in 700 μL of D_2O (99.96%, Sigma). One-dimensional ^1H nuclear magnetic resonance experiments were performed on a Varian VXR-500 spectrometer equipped with a 5 mm triple-resonance tunable probe with standard Varian software at 298 K.

The octasaccharide sample (50 μg) was dissolved in 40 μL of 5 mM sodium phosphate and 200 mM NaCl (pH 7.0). Heparin lyase I (1 unit) was applied for 24 h at 30 °C to ensure complete digestion of the sample. After the reaction was complete, the sample was heated at 100 °C for 1 min to inactivate the enzyme. The digestion product was compared to disaccharide standards using analytical SAX-HPLC to confirm identity (*22*).

Biotinylation of Peptidoglycan Heparin. Semipurified (unbleached) heparin is a mixture containing ~90% glycosaminoglycan and ~10% peptidoglycan heparin (*43*). Semipurified heparin (10 mg, Celsus Laboratories, Inc., Cincinnati, OH) was biotinylated in the core peptide using NHS-LC-biotin to afford reducing end biotinylated heparin. The position of the biotin on the peptide was confirmed through β-elimination, which selectively removed biotin, affording glycosaminoglycan heparin (*43*).

Preparation of Biosensor Chips. A heparin chip was prepared by immobilizing biotinylated heparin on a streptavidin sensor chip (Biacore) as described previously (*45*). The first three flow cells of the chip were treated with biotinylated heparin, while the fourth served as a control.

An apoE biochip was prepared by covalent attachment of the apoE4 N-terminal domain to the sensor surface through its primary amino groups. The carboxymethylated dextran surface (CM-5% sensor chip) was first activated with an injection pulse (7 min, 35 μL) of an equimolar mix of *N*-hydroxysuccinimide (NHS) and *N*-ethyl-*N*-[(dimethylamino)propyl]carbodiimide (final concentration of 0.05 M, mixed immediately before injection). The protein solution, 80 μL, was then injected manually (100 μg/mL in citrate buffer at pH 4.5). Four different pH values (4.5, 5, 5.5, and 6) were examined. A pH of 4.5 resulted in the immobilization of the greatest amount of apoE4. Excess unreacted sites on the sensor surface were blocked with a 35 μL injection of 1 M ethanolamine, and the surface was again cleaned with the extraclean program.

Kinetic Binding Measurements by Surface Plasmon Resonance (SPR). For the heparin chip, a 15 μL injection of apoE (concentration of 2.3−0.11 μM in 20 mM ammonium bicarbonate buffer at pH 7.4) was carried out at a flow rate of 5 μL/min. At the end of the sample plug, the same buffer was passed over the sensor surface to facilitate dissociation. After a suitable dissociation time, the sensor surface was regenerated for the next sample with a 10 μL pulse of 2 M NaCl. The response was monitored as a function of time (sensogram) at 25 °C.

For the apoE chip, a 15 μL injection of the HP octasaccharide (over a concentration range of 2.17−32.50 μM in 20 mM ammonium bicarbonate buffer at pH 7.4) was made at a flow rate of 5 μL/min. At the end of the sample plug, the same buffer was passed over the sensor surface to facilitate dissociation. After a suitable dissociation time, the sensor surface was regenerated for the next sample with a 10 μL pulse of 2 M NaCl. The response was monitored as a function of time (sensogram) at 25 °C. This procedure was repeated with full-length (14 800 Da) porcine intestinal mucosal heparin (Celsus Laboratories, Inc.) over a concentration range of 73−684 nM in 20 mM ammonium bicarbonate buffer at pH 7.4. Kinetic parameters were evaluated with BIA Evaluation software (version 3.0.2, 1999).

Isothermal Titration Calorimetry (ITC) Used To Assess the Octasaccharide−ApoE Interaction. ITC was performed on a microtitration calorimeter (Hart Scientific) to assess the interaction between the N-terminal fragment of apoE and the octasaccharide. The N-terminal apoE4 fragment (1.3 mL at 50 μM) was titrated with 18 injections (10 μL) of 1 mM octasaccharide. The samples were in 20 mM ammonium bicarbonate buffer (pH 7.4). The experiments were performed at 25 °C. Peak areas were analyzed with the BindWorks (version 1) program from Applied Thermodynamics. Experimental procedures and data fitting have been previously described (*23*).

Fluorescence Used To Assess the Octasaccharide−ApoE Interaction. The excitation wavelength was set at 295 nm, and the emission was measured from 300 to 400 nm. The titration was performed at 25 °C by adding small amounts (1−10 μL) of an octasaccharide solution (20 μM) into 500 μL of apoE (0.15 μM in 20 mM ammonium bicarbonate buffer at pH 7.4). An increase in fluorescence was observed at 353 nm with increasing octasaccharide concentrations. The increase in fluorescence at 353 nm typically results from the exposure of a tryptophan to solvent (*24*). A K_d was calculated from the resulting titration curve.

Determination of the High-Resolution Crystal Structure of ApoE4. Expression and purification of the 22 kDa N-terminal fragment of apoE4 have been described previously (*25*). Crystals were grown by vapor diffusion with the hanging drop method. The crystallization conditions were 22% polyethylene glycol 400 (Fluka), 20 mM sodium acetate (pH 6.2), and 0.1% β-mercaptoethanol. One month before data collection, the concentration of polyethylene glycol 400 in the reservoir solution was increased to 28%. At the time of data collection, the crystals were mounted in a hair loop with the reservoir solution as the cryoprotectant. Data beyond 1.8 Å were collected on the Advanced Light Source beamline 5.0.2, equipped with an Oxford cryostream and a Quantum4 ADSC CCD detector. The data were integrated with MOSFILM (*26*) and scaled with SCALA (*27*). The structure was determined by molecular replacement with the model of apoE3 as determined by the multiple-anomalous dispersion method (1BZ4) (*28*) with all of the lysines, glutamates, glutamines, and arginines converted to alanine residues. After rigid-body refinement, as implemented in X-PLOR 3.8 (*29*), the initial R_{work} and R_{free} were 0.31 and 0.37, respectively. Omit electron density maps covering contiguous blocks of approximately 10% of the protein were generated with the wARP method (*30*). The model in each block was rebuilt with XTALVIEW (*31*). The models were refined through cycles of REFMAC (*32*) and calculations of wARP maps and model rebuilding. The final model was polished with cycles of omit maps, model building, and refinement with X-PLOR. The deviations from ideal values for the bond distances and angles and the final *R*-factors are summarized in Table 1. The final model was checked with the program

Table 1: Statistics for Data Collection and Refinement of the 22 kDa N-Terminal Fragment of ApoE4

data collection statistics	
space group	$P2_12_12_1$
cell constants (Å)	40.22, 53.21, 84.76
resolution (Å)	1.8
overall completeness (%)	99.1
overall $\langle I/\sigma(I)\rangle$	27.4
overall R_{merge}	0.037
resolution of the highest shell (Å)	1.80−1.98
completeness of the highest shell (%)	98.7
$\langle I/\sigma(I)\rangle$ of the highest shell	3.7
R_{merge} of the highest shell	0.199
refinement statistics	
resolution (Å)	1.8
no. of unique reflections	15844
no. of non-hydrogen protein atoms	1142[a]
deviations from ideality	
bond lengths (Å)	0.004
bond angles (deg)	0.8
R_{work}	0.226[b]
R_{free}	0.230

[a] There was insufficient electron density to locate residues 1−22, 84, 85, and 163−191 in the final electron density maps. [b] The final model was the result of the refinement cycle in which R_{work} and R_{free} were the closest. Although further refinement decreased R_{work} to <0.20, it did not significantly decrease R_{free}, indicating that the no further improvement in the phases was obtained by continuing the refinement past this point.

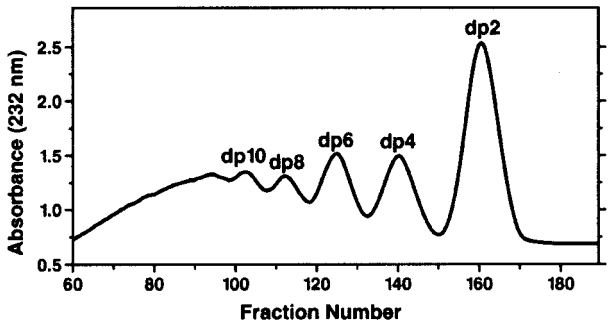

FIGURE 1: Gel filtration of heparin-derived oligosaccharides. Heparin was partially depolymerized with heparin lyase I and fractionated by size on a Sephadex G-50 column. Peaks corresponding to disaccharide (dp2), tetrasaccharide (dp4), hexasaccharide (dp6), and octasaccharide (dp8) were collected and desalted.

WHATIF and deposited with the Protein Data Bank (entry 1B68).

RESULTS

Heparin was subjected to controlled enzymatic depolymerization and pressure filtration to yield a mixture of oligosaccharides ranging from disaccharide [degree of polymerization (dp) 2] to tetradecasaccharide (dp14). The high-molecular weight oligosaccharides (M_r > 5000) were removed by pressure filtration. Separation of the low-molecular weight oligosaccharide mixture (M_r < 5000) on Sephadex G-50 yielded oligosaccharide fractions (Figure 1). The tetrasaccharide-, hexasaccharide-, and octasaccharide-sized fractions were next examined for affinity for the immobilized apoE4 N-terminal domain. The tetrasaccharide fraction exhibited no interaction, while the hexasaccharide and octasaccharide fractions displayed oligosaccharides that bound to the affinity column. SAX-HPLC analysis and apoE affinity fractionation showed that the hexasaccharide mixture contained two interacting oligosaccharides (not shown),

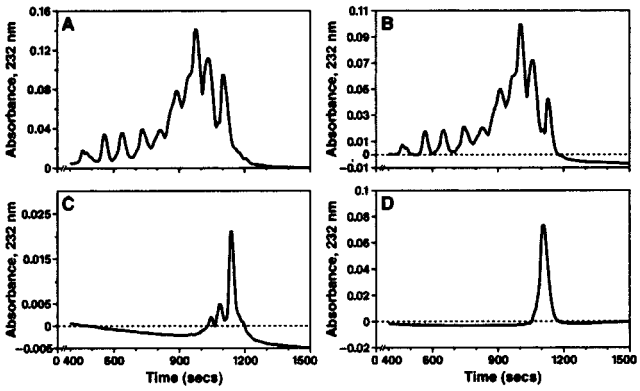

FIGURE 2: Isolation of an octasaccharide by affinity chromatography. The heparin octasaccharide fraction from the Sephadex G-50 column (Figure 1) was applied to an affinity matrix on which the N-terminal domain of apoE4 was immobilized. Fractions were analyzed by analytical SAX-HPLC: (A) the octasaccharide (dp8) fraction from Figure 1, (B) the octasaccharide flow-through fraction from the apoE affinity column, (C) the high-affinity octasaccharide fraction from the apoE affinity column containing a single major peak at 1100 s, and (D) the octasaccharide purified from the octasaccharide fraction by preparative SAX-HPLC. Peaks eluting before 400 s correspond to the injection front.

whereas the octasaccharide mixture exhibited only a single interacting oligosaccharide (Figure 2). The two peaks in the hexasaccharide fraction showing affinity for apoE were identified as ΔUAp2S(1→[4)-α-D-GlcNpS6S(1→4)-α-L-IdoAp2S(1→]$_2$4)-α-D-GlcNpS6S and ΔUAp2S(1→4)-α-D-GlcNpS6S(1→4)-α-L-IdoAp2S(1→4)-α-D-GlcNpS6S(1→4)-β-D-GlcAp(1→4)-α-D-GlcNpS6S, by coelution via SAX-HPLC with standards previously prepared in our laboratory (*20*). The peak corresponding to the high-affinity binding octasaccharide was identified in the octasaccharide-sized fraction by co-injection on analytical SAX-HPLC. Repetitive SAX-HPLC of the octasaccharide mixture yielded multimilligram quantities of this high-affinity binding octasaccharide for structural characterization and interaction studies.

Structural Characterization of the Oligosaccharide. Analysis of the isolated oligosaccharide by CE gave a single major peak at a migration time of 400 s (Figure 3A). The presence of a single major symmetrical peak confirmed that the sample is >95% pure. Polyacrylamide gel electrophoresis analysis of the oligosaccharide showed it to be an octasaccharide (Figure 3B). Heparin lyase I cleaves heparin endolytically at the →4)-α-D-GlcNpS6S(1→4)-α-L-IdoAp2S(1→ linkage (*33*), the most frequently occurring glucosaminidic linkage. Thus, an oligosaccharide consisting only of repeats of the major disaccharide unit of heparin should be completely depolymerized to the disaccharide by treatment with heparin lyase I. Analysis of the digestion products of the oligosaccharide on SAX-HPLC yielded a single symmetrical peak at 27 min (Figure 3C). This peak corresponds to the retention time of the disaccharide standard from heparin, ΔUAp2S-(1→4)-D-GlcNpS6S, previously characterized in our laboratory (*34*). One-dimensional ^{1}H nuclear magnetic resonance spectroscopy was used to confirm that the identity of the oligosaccharide is the fully sulfated heparin octasaccharide of the structure, ΔUAp2S(1→[4)-α-D-GlcNpS6S(1→4)-α-L-IdoAp2S(1→]$_3$4)-α-D-GlcNpS6S (Table 2).

SPR Studies. Peptidoglycan heparin, biotinylated on the peptide at its reducing end, was immobilized on the surface of a streptavidin-coated sensor chip. Immobilization was

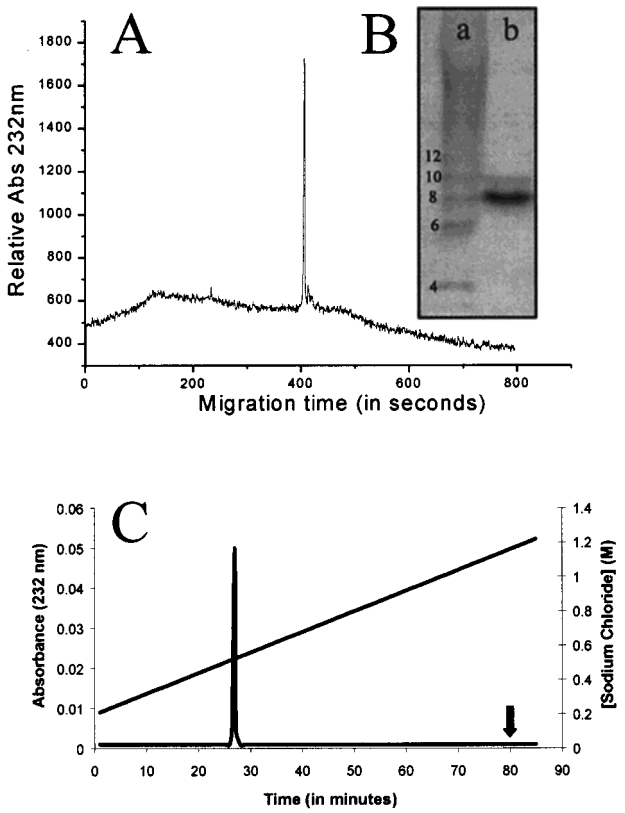

FIGURE 3: Structural characterization of the heparin octasaccharide with high affinity for the apoE4 N-terminal domain. (A) Capillary electrophoresis of the octasaccharide indicated that it is >95% pure. (B) Analysis of the octasaccharide by polyacrylamide gel electrophoresis: lane a, ladder of heparin-derived oligosaccharide standards with the dp of intense bands marked; and lane b, purified heparin octasaccharide. (C) Analytical SAX-HPLC chromatogram of the octasaccharide after exhaustive depolymerization with heparin lyase I. The observed peak coelutes with a disaccharide standard with the structure ΔUAp2S(1→4)-D-GlcNpS6S. The arrow indicates the position where the heparin octasaccharide eluted before treatment with heparin lyase I.

Table 2: ^{1}H NMR Spectral Characteristics of the Heparin Octasaccharide Chemical Shift in Parts per Million and Integration

	ΔUAp2S	GlcNpS6S	IdoAp2S
H1	5.51 (1H)	5.36−5.42 (4H)	5.26−5.31 (3H)
H2	4.59 (1H)	3.24−3.30 (4H)	4.30−4.33 (3H)
H3	4.32 (1H)	3.68−3.72 (4H)	4.18−4.22 (3H)
H4	5.96 (1H)	3.79−3.83 (4H)	4.08−4.13 (3H)
H5		3.98−4.06 (4H)	4.77−4.82 (3H)
H6a		4.33−4.39 (4H)	
H6b		4.23−4.28 (4H)	

confirmed by an increase of 1000 RU (response unit) on the sensor chip. Biotinylated heparin was stably bound to the sensor surface. Even after 10 injections of apoE and 10 regeneration steps with 2 M NaCl, more than 90% of the reactivity remained.

Several concentrations of apoE were injected over the biochip containing immobilized heparin to estimate the rate constants and affinity parameters of the apoE−heparin interaction (Figure 4A). Both the association and dissociation kinetics fitted a one-site model, and the on-rate (k_{on}), off-rate (k_{off}), and dissociation constants for this interaction are given in Table 3.

Since the heparin octasaccharide is too small to immobilize onto a sensor chip, we next immobilized apoE on the

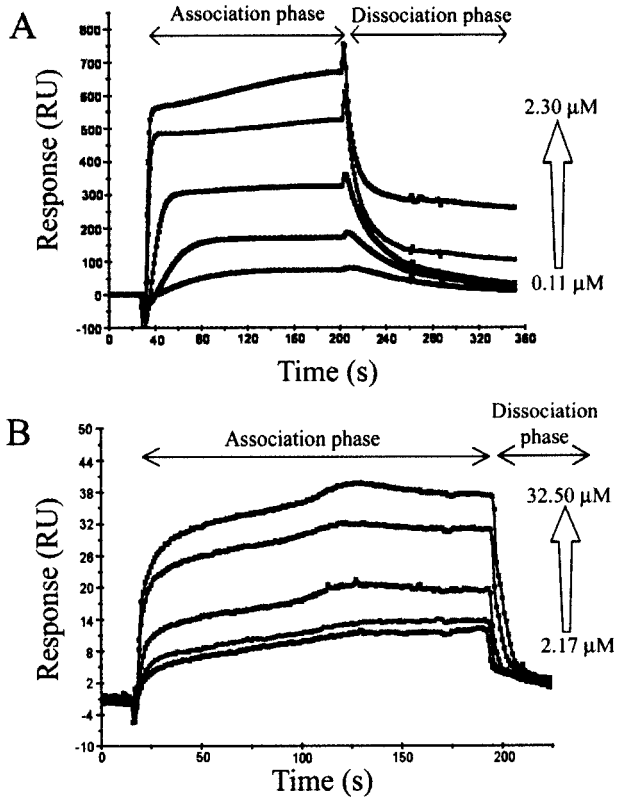

FIGURE 4: SPR data on the interaction of the apoE4 N-terminal domain with heparin and heparin octasaccharide. (A) SPR sensograms of apoE4 N-terminal domain interacting with immobilized heparin. The apoE4 N-terminal domain at 0.11, 0.23, 0.91, 1.37, and 2.28 μM was passed over a Biacore chip containing immobilized heparin. (B) SPR sensograms of the heparin octasaccharide with the immobilized N-terminal domain of apoE4. Heparin octasaccharide at 2.17, 4.07, 8.23, 16.46, and 32.50 μM was passed over a Biacore chip containing the immobilized N-terminal domain of apoE4.

Table 3: Binding of the N-Terminal Domain of ApoE4 to Heparin and Octasaccharide As Determined by SPR

	k_{on} (M^{-1} s^{-1})	k_{off} (s^{-1})	K_D (nM)
heparin[a]	8.4×10^4	1.3×10^{-2}	150
octasaccharide[b]	1.5×10^5	2.0×10^{-2}	133
heparin[b]	7.4×10^4	9.6×10^{-4}	13

[a] ApoE4 (N-terminal domain) flowed over reducing end immobilized heparin. [b] Heparin or octasaccharide flowed over the immobilized N-terminal domain of apoE4.

negatively charged carboxymethylated dextran sensor surface of a plasmon resonance chip to examine binding in the reverse configuration. The heparin octasaccharide exhibited a strong interaction when passed over the apoE surface (Figure 4B). Both the association and dissociation rate constants fit well to a single-site model, affording k_{on}, k_{off}, and K_d values for the interaction between apoE and the heparin octasaccharide (Table 3). As a control experiment, heparin was passed over the apoE surface. We observed a k_{on} comparable to that observed for the octasaccharide; however, the k_{off} was significantly lower, giving a 10-fold lower K_d (Table 3). The data for heparin interaction with immobilized apoE fit best to a bivalent analyte model, suggesting that heparin makes more than one contact with the immobilized apoE molecules on the chip surface, complicating the direct comparison of these data to those obtained for the octasaccharide.

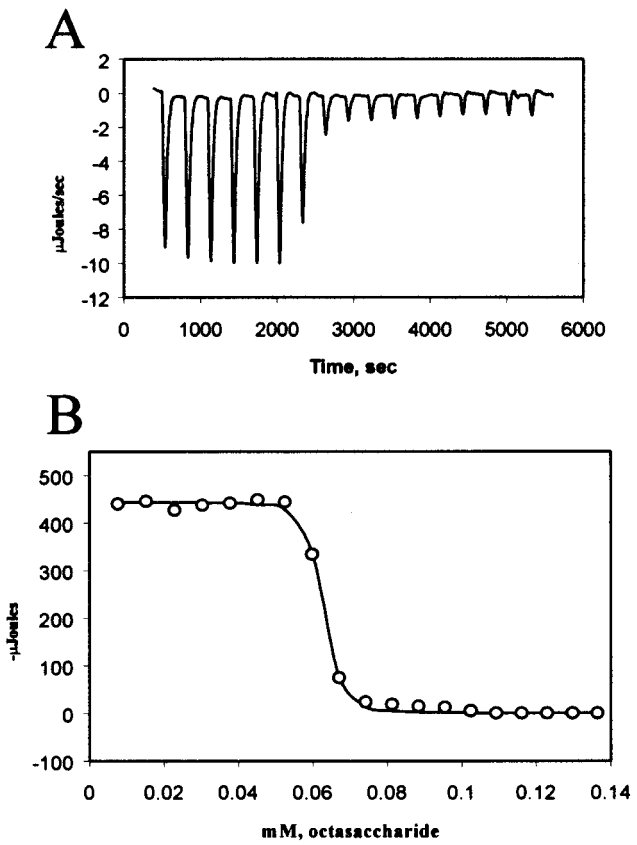

FIGURE 5: ITC analysis of the heparin octasaccharide that interacts with the N-terminal domain of apoE4. (A) The heat evolved as a function of time is shown over the course of 18 injections (10 μL) of the heparin octasaccharide into 1.3 mL of apoE4 (50 μM). (B) Integrated data, with heat in microjoules (peak area in panel A) as a function of heparin octasaccharide concentration. The fitted data (—) describe an interaction with a ΔH of −44 kcal/mol, a K_d of 76 nM, and a stoichiometry (n) of 1.26 molecules of octasaccharide per molecule of apoE.

ITC Studies. The binding of the N-terminal apoE4 fragment to the fully sulfated octasaccharide was determined by ITC. The heats of titration (Figure 5) were measured, and the fitted data describe an interaction with a ΔH of −44 kcal/mol, a K_d of 76 nM, and a stoichiometry (n) of 1.26 molecules of octasaccharide per protein.

Fluorescence Studies. The binding of the N-terminal fragment of apoE4 with the heparin octasaccharide was also studied by fluorescence spectroscopy. An increase in fluorescence at 353 nm was observed on titration of apoE4 with the octasaccharide (data not shown). A K_d of ∼1 μM was calculated from the resulting titration curve.

DISCUSSION

Studies on the interaction of apoE4 and heparin were undertaken because of the demonstrated importance of the apoE interaction with HSPGs in lipoprotein remnant clearance and the potential importance of the interaction of apoE4 with the heparin-related proteoglycan heparan sulfate in the pathogenesis of Alzheimer's disease. Heparin oligosaccharides, prepared by treating heparin with heparin lyase I, have been purified and structurally characterized (*20*). Using this enzymatic approach, we prepared a mixture of heparin oligosaccharides and fractionated it by gel permeation chromatography to obtain oligosaccharide fractions of uniform size. Tetrasaccharide (dp4), hexasaccharide (dp6), and octasaccharide (dp8) fractions were screened for their interactions with an affinity matrix containing the immobilized apoE4 N-terminal domain. The apoE4 N-terminal domain was selected for this study because it contains a heparin-binding site (*16*) characterized by basic residues that play a major role in heparin binding (Figure 6). This fragment also contains a Cardin−Weintraub heparin-binding sequence (*35*).

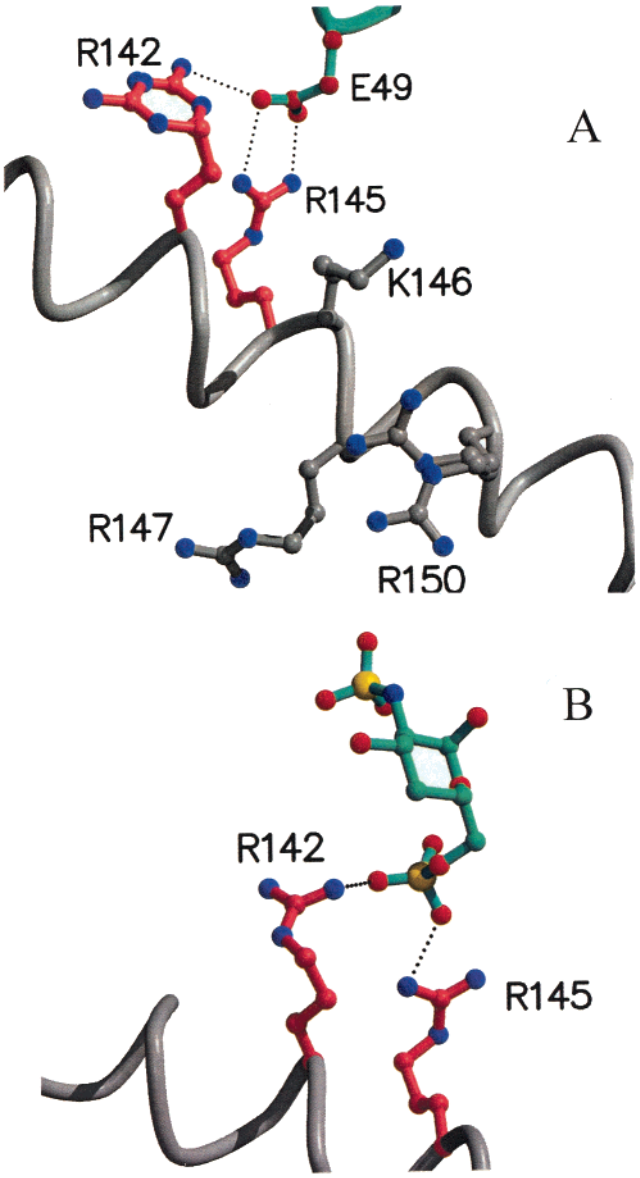

FIGURE 6: Model of heparin binding to apoE. (A) The heparin-binding site (residues 142−150) in the 1.8 Å crystal structure of the 22 kDa N-terminal domain of apoE4 (PDB entry 1B68). In the crystal structure, the R142 and R145 side chains (pink) form cell contacts with E49 (cyan) from an adjacent symmetry-related molecule. The A and B conformations of both R142 and R150 are shown. For all side chains, the oxygen atoms are shown in red and the nitrogen atoms are shown in blue. (B) Model of the R142 and R145 anion binding site that forms two salt bridges with the 6-*O*-sulfo group of glucosamine.

The tetrasaccharide mixture did not interact when passed through an apoE4 affinity matrix in a buffer containing 150 mM sodium chloride, suggesting that such oligosaccharides were of insufficient size to promote strong binding to apoE. We next fractionated the hexasaccharide (dp6) fraction by

affinity chromatography. SAX-HPLC analysis of this fraction showed that it contained two interacting oligosaccharides, suggesting a lack of selectivity in these interactions. The binding of hexasaccharides, the octasaccharide, and heparin to the apoE4 N-terminal domain, as measured by affinity chromatography, exhibited elution over a narrow range of sodium chloride concentrations (from 0.2 to 0.5 M), limiting the utility of this method for a detailed study of these interactions.

The octasaccharide (dp8) fraction was examined in detail as it contained a single oligosaccharide that bound apoE4 with sufficient avidity to result in a selective interaction. SAX-HPLC was used to prepare multi-milligram amounts of this high-affinity oligosaccharide from the octasaccharide fraction. CE analysis demonstrated that the oligosaccharide was >95% pure, and PAGE analysis confirmed that it was an octasaccharide. Exhaustive treatment of this octasaccharide with heparin lyase I afforded a single product that coeluted on analytical SAX-HPLC with the disulfated disaccharide, ΔUAp2S(1→4)-α-D-GlcNpS6S. ^{1}H nuclear magnetic resonance spectroscopy of the high-affinity heparin octasaccharide (Table 2) was used to confirm its structure as ΔUAp2S(1→[4)-α-D-GlcNpS6S(1→4)-α-L-IdoAp2S(1→]$_3$4)-α-D-GlcNpS6S. This was identical to a heparin octasaccharide previously prepared and characterized in our laboratory (*20*). It is important to note that the natural ligand for apoE4 is probably heparan sulfate. The isolation of a heparin octasaccharide suggests that a sequence within heparan sulfate of similar size, but probably having a lower level of sulfation, corresponds to the binding partner for apoE4. On average, heparan sulfate has a significantly lower level of sulfation than heparin (*17*, *18*). However, the most common disaccharide isolated from liver heparan sulfate has the same pattern of sulfation as the disaccharide sequence in the heparin octasaccharide fragment (→4)-α-L-IdoAp2S-(1→4)-α-D-GlcNpS6S) (*46*). Therefore, the physiological ligand of apoE may have a much higher degree of sulfation than heparan sulfate from other sources. It is also possible that not all the sulfate groups, present in the heparin octasaccharide fragment, may be required by the endogenous ligand for binding apoE4. For example, in the case of the fibroblast growth factor 2 (FGF-2)−heparin interaction, the 6-*O*-sulfate groups on glucosamine residues of heparin are not required for heparan sulfate binding to FGF-2 (*47*).

In a recent study, Shuvaev and co-workers studied the interaction of apoE and heparin by SPR spectroscopy (*36*). They found a K_d of ∼10 nM for the interaction of heparin (or heparan sulfate) with full-length apoE under the same experimental conditions used in the current study. Furthermore, these investigators demonstrated that a heparin pentasaccharide could competitively interfere with the heparin−apoE interaction but bound apoE with considerably less avidity than did heparin. Our studies assessing the interaction of the apoE4 N-terminal domain with immobilized heparin demonstrated binding (K_d = 150 nM) that was weaker than that observed with full-length apoE. The difference in interaction between the N-terminal domain and full-length apoE appears to be primarily due to the faster (100-fold) off-rate observed in the truncated structure, suggesting a secondary contact between the apoE C-terminal domain and heparin, which stabilizes this interaction once the initial contact is made. This possibility is consistent with the presence of one or more additional binding sites in the C-terminus of apoE (*16*). The interaction of the octasaccharide with the immobilized N-terminal fragment of apoE yielded twice the k_{on} and k_{off}, with essentially the same K_d, observed for the interaction with intact heparin (Table 3). The interaction of heparin with the immobilized N-terminal domain of apoE yielded a 10-fold lower K_d than the octasaccharide; however, comparison of these experiments is complicated by the fact that heparin can make more than one interaction with the immobilized apoE.

The thermodynamics of the binding of the octasaccharide to the 22 kDa N-terminal domain of apoE4 was next examined by ITC. A ΔH of −44 kcal/mol was observed for the binding interaction. From an analysis of the ITC data, a K_d of 76 nM and a stoichiometry of 1.26 mol of octasaccharide/mol of the apoE4 N-terminal domain were calculated. This stoichiometry supports the hypothesis that a single octasaccharide binds to the heparin-binding site in the N-terminal domain of apoE4. The most highly sulfated hexasaccharide having affinity for apoE4 was also examined by ITC. This hexasaccharide bound with considerably (1000-fold) lower affinity than the strongly interacting octasaccharide. These data together with the affinity chromatography and SPR experiments confirm that the isolated octasaccharide is the minimum sized binding partner required for strong interaction with the apoE4 N-terminal domain.

Previous studies have shown that the sequence of residues 136−150 contains both the low-density lipoprotein receptor and heparan sulfate proteoglycan binding sites and that the basic residues in this region are key to both interactions. To examine this region of apoE at higher resolution than is available with current models, we have improved the resolution of the model to 1.8 Å. Examination of this region reveals that there are two pairs of arginines positioned so that each pair forms an anion binding site: R142 and R145 and R147 and R150. In each case, the pair of arginines interacts with a glutamate from a symmetry-related molecule. For example, R145 forms two salt bridges: NH1 R145 and OE1 E49 and NH2 R145 and OE2 E49. The B conformation of R142 is also hydrogen bonded to one of the carboxyl oxygens of the same glutamate (NH R142 and OE E49) (Figure 6A). Although the observed conformations of R145 and R142 are an artifact of the crystal structure, they demonstrate that the guanidyl groups of R142 and R145 can form salt bridges with the same anion. R147 and R150 form similar interactions with E70 from a symmetry-related molecule. However, the near-normal heparin binding affinity of apoE2 (*37*) indicates that R150 is unlikely to form a direct interaction with the heparin fragment, since R150 has been shown to form a salt bridge with D154 in apoE2 (*38*, *39*).

To explore the potential role of the R142 and R145 pair in binding to heparin, we performed manual docking using the structures of heparin fragments deposited in the Protein Data Bank (*40*, *41*) with the N-terminal domain of apoE4. These results indicate that a dodecasaccharide fragment of heparin can be positioned so that either a 6-*O*-sulfo group from a glucosamine forms a salt bridge with both R142 and R145 (Figure 6B) or R142 and R145 form salt bridges with sulfates from adjacent saccharide residues. These orientations of the fragment result in the predicted formation of additional interactions between the heparin fragment and K143, K146, and R147 without any bad contacts with the N-terminal

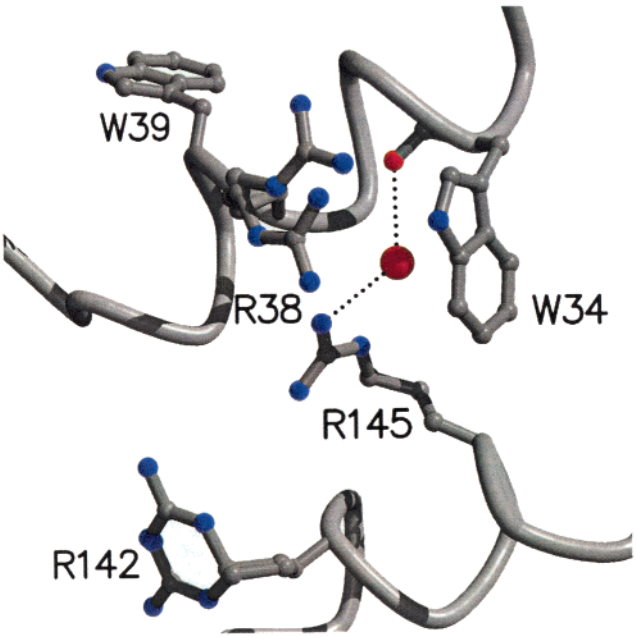

FIGURE 7: Relationship of R145 and W34 and the interactions that link R145 and W34 in the crystal structure of apoE4. The carbonyl oxygen of W34 is hydrogen bonded to the same water molecule (red ball) as R145. This water molecule is positioned directly beneath the plane of the tryptophan side chain so that release of this water molecule through disruption of its hydrogen bond with R145 should affect the fluorescence of W34. In addition, the fluorescence of W39 may also be affected by heparin binding. The A conformation of the guanidyl group of R38 is 3.67 Å from the guanidyl group of R145, and W39 is directly adjacent to R38. In this figure, both the A and B conformations of R38 and R142 are shown.

domain of apoE4. The hypothesis that R142 and R145 form salt bridges with sulfate groups from the octasaccharide fragment is consistent with the heparin-binding activities of the R142C apoE4 and R145C apoE4 mutants. Both of these mutants have a dramatically reduced binding affinity for HSPGs (*42*).

To test the hypothesis that R145 binds directly to the octasaccharide heparin fragment, we measured the change in apoE fluorescence upon heparin binding. While a change in fluorescent intensity has been reported for the binding of antithrombin III to its heparin pentasaccharide (*24*), there are no similar reports of changes in apoE fluorescence on heparin binding. Although there are eight fluorescent residues in the 22 kDa fragment of apoE4, only two (W34 and W39) are close enough to the putative heparin-binding site to be significantly affected by the binding of heparin to R145 (Figure 7). The other two tryptophans and the four tyrosines in the N-terminal domain of apoE4 are more than 10 Å from the residues in the heparin-binding site in helix 4. Titration of the N-terminal domain of apoE4 with the high-affinity binding octasaccharide afforded an increase in tryptophan fluorescence corresponding to a K_d of 1 μM, but no significant changes in tyrosine fluorescence. The K_d observed by fluorescence, while higher than that observed by ITC and SPR, is well within the expected variability observed in K_d measurements taken by different experimental techniques (*44*). Studies are currently focused on the cocrystallization of the N-terminal domain of apoE4 with the high-affinity binding heparin octasaccharide. The X-ray crystal structure of this complex should reveal the exact position of the heparin-binding site in the apoE4 N-terminal domain.

ACKNOWLEDGMENT

We thank John W. C. Carroll for graphics arts, Brian Auerbach for manuscript preparation, Stephen Ordway and Gary Howard for editorial assistance, and Mark Knapp for his help processing the X-ray data.

REFERENCES

1. Weisgraber, K. H., and Mahley, R. W. (1996) *FASEB J. 10*, 1485−1494.
2. Mahley, R. W., and Rall, S. C., Jr. (1995) in *The Metabolic and Molecular Bases of Inherited Disease* (Scriver, C. R., Beaudet, A. L., Sly, W. S., and Valle, D., Eds.) 7th ed., pp 1953−1980, McGraw-Hill, New York.
3. Luc, G., Bard, J.-M., Arveiler, D., Evans, A., Cambou, J.-P., Bingham, A., Amouyel, P., Schaffer, P., Ruidavets, J.-B., Cambien, F., Fruchart, J.-C., and Ducimetiere, P. (1994) *Arterioscler. Thromb. 14*, 1412−1419.
4. Davignon, J., Cohn, J. S., Mabile, L., and Bernier, L. (1999) *Clin. Chim. Acta 286*, 115−143.
5. Corder, E. H., Saunders, A. M., Risch, N. J., Strittmatter, W. J., Schmechel, D. E., Gaskell, P. C., Jr., Rimmler, J. B., Locke, P. A., Conneally, P. M., Schmader, K. E., Small, G. W., Roses, A. D., Haines, J. L., and Pericak-Vance, M. A. (1994) *Nat. Genet. 7*, 180−184.
6. Saunders, A. M., Strittmatter, W. J., Schmechel, D., St. George-Hyslop, P. H., Pericak-Vance, M. A., Joo, S. H., Rosi, B. L., Gusella, J. F., Crapper-MacLachlan, D. R., Alberts, M. J., Hulette, C., Crain, B., Goldgaber, D., and Roses, A. D. (1993) *Neurology 43*, 1467−1472.
7. Strittmatter, W. J., Saunders, A. M., Schmechel, D., Pericak-Vance, M., Enghild, J., Salvesen, G. S., and Roses, A. D. (1993) *Proc. Natl. Acad. Sci. U.S.A. 90*, 1977−1981.
8. Aggerbeck, L. P., Wetterau, J. R., Weisgraber, K. H., Wu, C.-S. C., and Lindgren, F. T. (1988) *J. Biol. Chem. 263*, 6249−6258.
9. Wetterau, J. R., Aggerbeck, L. P., Rall, S. C., Jr., and Weisgraber, K. H. (1988) *J. Biol. Chem. 263*, 6240−6248.
10. Wilson, C., Wardell, M. R., Weisgraber, K. H., Mahley, R. W., and Agard, D. A. (1991) *Science 252*, 1817−1822.
11. Weisgraber, K. H. (1994) *Adv. Protein Chem. 45*, 249−302.
12. Mahley, R. W. (1988) *Science 240*, 622−630.
13. Rall, S. C., Jr., Weisgraber, K. H., and Mahley, R. W. (1982) *J. Biol. Chem. 257*, 4171−4178.
14. Dong, L.-M., Wilson, C., Wardell, M. R., Simmons, T., Mahley, R. W., Weisgraber, K. H., and Agard, D. A. (1994) *J. Biol. Chem. 269*, 22358−22365.
15. Cardin, A. D., Hirose, N., Blankenship, D. T., Jackson, R. L., and Harmony, J. A. K. (1986) *Biochem. Biophys. Res. Commun. 134*, 783−789.
16. Weisgraber, K. H., Rall, S. C., Jr., Mahley, R. W., Milne, R. W., Marcel, Y. L., and Sparrow, J. T. (1986) *J. Biol. Chem. 261*, 2068−2076.
17. Hileman, R. E., Fromm, J. R., Weiler, J. M., and Linhardt, R. J. (1998) *BioEssays 20*, 156−167.
18. Linhardt, R. J., and Toida, T. (1997) in *Carbohydrates as Drugs* (Witczak, Z. B., and Nieforth, K. A., Eds.) pp 277−341, Marcel Dekker, New York.
19. Mahley, R. W., and Ji, Z.-S. (1999) *J. Lipid Res. 40*, 1−16.
20. Pervin, A., Gallo, C., Jandik, K., Han, X.-J., and Linhardt, R. J. (1995) *Glycobiology 5*, 83−95.
21. Pervin, A., Al-Hakim, A., and Linhardt, R. J. (1994) *Anal. Biochem. 221*, 182−188.
22. Rice, K. G., Kim, Y. S., Grant, A. C., Merchant, Z. M., and Linhardt, R. J. (1985) *Anal. Biochem. 150*, 325−331.
23. Hileman, R. E., Jennings, R. N., and Linhardt, R. J. (1998) *Biochemistry 37*, 15231−152317.
24. Desai, U. R., Petitou, M., Björk, I., and Olson, S. T. (1998) *J. Biol. Chem. 273*, 7478−7487.

25. Morrow, J. A., Arnold, K. S., and Weisgraber, K. H. (1999) *Protein Expression Purif. 16*, 224−230.
26. Leslie, A. G. W. (1992) in *CCP4 and ESF-EACMB Newsletter on Protein Crystallography*, p 26, Cambridge Collaborative Project 4, Daresbury, England.
27. Kabsch, W. (1988) *J. Appl. Crystallogr. 21*, 916−924.
28. Segelke, B. W., Forstner, M., Knapp, M., Trakhanov, S. D., Parkin, S., Newhouse, Y. M., Bellamy, H. D., Weisgraber, K. H., and Rupp, B. (2000) *Protein Sci. 9*, 886−897.
29. Brünger, A. T. (1992) *X-PLOR, Version 3.1. A System for X-ray Crystallography and NMR*, Yale University Press, New Haven.
30. Perrakis, A., Sixma, T. K., Wilson, K. S., and Lamzin, V. S. (1997) *Acta Crystallogr. D53*, 448−455.
31. McRee, D. E. (1992) *J. Mol. Graphics 10*, 44−46.
32. Murshudov, G. N., Vagin, A. A., and Dodson, E. J. (1997) *Acta Crystallogr. D53*, 240.
33. Jandik, K. A., Gu, K., and Linhardt, R. J. (1994) *Glycobiology 4*, 289−296.
34. Merchant, Z. M., Kim, Y. S., Rice, K. G., and Linhardt, R. J. (1985) *Biochem. J. 229*, 369−377.
35. Cardin, A. D., and Weintraub, H. J. (1989) *Arteriosclerosis 9*, 21−32.
36. Shuvaev, V. V., Laffont, I., and Siest, G. (1999) *FEBS Lett. 459*, 353−357.
37. Horie, Y., Fazio, S., Westerlund, J. R., Weisgraber, K. H., and Rall, S. C., Jr. (1992) *J. Biol. Chem. 267*, 1962−1968.
38. Wilson, C., Mau, T., Weisgraber, K. H., Wardell, M. R., Mahley, R. W., and Agard, D. A. (1994) *Structure 2*, 713−718.
39. Dong, L.-M., Parkin, S., Trakhanov, S. D., Rupp, B., Simmons, T., Arnold, K. S., Newhouse, Y. M., Innerarity, T. L., and Weisgraber, K. H. (1996) *Nat. Struct. Biol. 3*, 718−722.
40. Mikhailov, D., Linhardt, R. J., and Mayo, K. H. (1997) *Biochem. J. 328*, 51−61.
41. Mulloy, B., Forster, M. J., Jones, C., and Davies, D. B. (1993) *Biochem. J. 293*, 849−858.
42. Ji, Z.-S., Fazio, S., and Mahley, R. W. (1994) *J. Biol. Chem. 269*, 13421−13428.
43. Liu, J., Desai, U. R., Han, X., Toida, T., and Linhardt, R. J. (1995) *Glycobiology 5*, 765−774.
44. Connors, K. A. (1987) in *Binding Constants, The Measurement of Molecular Complex Stability*, pp 363−372, John Wiley & Sons, New York.
45. Capila, I., VanderNoot, V. A., Mealy, T. R., Seaton, B. A., and Linhardt, R. J. (1999) *FEBS Lett. 446*, 327−330.
46. Lyon, M., Deakin, J. A., and Gallagher, J. T. (1994) *J. Biol. Chem. 269*, 11208−11215.
47. Faham, S., Linhardt, R. J., and Rees, D. C. (1998) *Curr. Opin. Struct. Biol. 8*, 578−586.

BI002417N